Correlation of Ac-Impedance and In Situ X-ray Spectra of $LiCoO_2$

Francesco Nobili,[†] Sonia Dsoke,[†] Marco Minicucci,[‡] Fausto Croce,*[,§] and Roberto Marassi*[,†]

Dipartimento di Scienze Chimiche, Università di Camerino. Via S. Agostino 1, Camerino 62032, Italy, Centro Interdipartimentale Grandi Apparecchiature, Camerino, Italy, and Dipartimento di Scienze del Farmaco, Università degli Studi "G. D'Annunzio", Chieti 66013, Italy.

Received: January 30, 2006; In Final Form: March 14, 2006

In-situ X-ray and AC-impedance spectra have been obtained simultaneously during the deintercalation of lithium from $LiCoO_2$ using a specially designed electrochemical cell. The AC-dispersions have been correlated with the cell parameters obtained from the X-ray spectra. The correlation confirms previous hypothesis on the interpretation of the AC-dispersions in terms of an equivalent circuit comprising an element that relates the change of the intrinsic electronic conductivity, occurring at the early stages of deintercalation, to the semiconductor to metal transition caused by the change of the cell parameters.

Introduction

Mixed oxides of Li and transition metals belonging to the fourth row of the periodic table, of general formula $LiCo_yNi_{1-y}O_2$, are materials of great interest for the preparation of cathodes for lithium-ion rechargeable batteries.[1−10]

Despite the wide use of these materials, and particularly of $LiCoO_2$, that is the most commonly used cathode in lithium-ion cells, there is still some debate about the interpretation of the AC-dispersions at high intercalation degrees (x in Li_xCoO_2 between 1 and 0.9). At values of x close to unity the AC-spectra are dominated by a great semicircular arc in the low frequency region that is strongly potential dependent and shows an increasing tendency to close on the real axis with decreasing x. Some authors tried to explain this arc as due to a capacitive behavior of the electrodes,[11] while some others justify the high impedance as due to kinetic limitations related to the exchange current.[12] In previous papers[13−16] we have studied the ac-impedance spectra of compounds of the family $LiCo_yNi_{1-y}O_2$, devoting special emphasis to their ionic and electronic transport properties. It has been shown that the insulator-to-metal transition[17,18] characteristic of the early stages of the deintercalation in $LiCoO_2$ and, to a lesser extent, in the mixed $LiCo_yNi_{1-y}O_2$ compounds, is reflected in the AC impedance spectra. The evolution with x of the resistance associated with the low frequency arc closely resembles the variation of the electronic conductivity of the material as reported by Shibuya et al. for the same compound.[19] Taking this into account, the arc has been attributed to the variation of the electronic properties of the material during the Li deintercalation process, and the overall impedance dispersion has been interpreted on the basis of an equivalent circuit including an RQ parallel (where Q is the constant phase element defined in ref 20) related to the electronic conductivity. The EIS spectra of Li_xCoO_2 electrodes taken at different temperatures confirm this hypothesis. The apparent electronic conductivity (1/R) is thermally activated with activation energies that drop from about 0.4 eV for $x \cong 1$ to about 0.1 at $x \cong 0.9$ to become practically 0 at $x = 0.53$ when the material is metallic.[16]

Literature data, both experimental and theoretical,[17−19,21−29] agree about the existence of a link between the electronic structure of the oxides and their electronic and electrochemical properties. Goodenough[30] and Molenda et al.[31−33] developed an empirical model in which layered intercalation compounds of the general chemical formula A_xMX_2 (A = Li, Na; M = V, Cr, Mn, Co, Ni; X = O, S, Se) and crystallographic space group R-3m can be grouped in two classes on the basis of the in-plane R_{M-M} distance in the $(MX_2)_n$ layers that form the host structure of the lattice (this distance corresponds to the cell parameter a). When the R_{M-M} distance is higher than a critical value R_C, that depends on the composition of the material, the compound behaves as an insulator. When the distance is lower than R_C, the material presents metallic type behavior because the overlapping of the localized atomic t_{2g} orbital leads to the formation of a conduction band. In the case of Li_xCoO_2 compounds, Ménétrier et al.[22] have pointed out that the Co−Co distance is smaller than the critical R_C value whatever the lithium amount. This means that electronic delocalization should be expected. However, in lithium rich solid solutions the number of Co(IV) ions (holes in the t_{2g} band) is too low to lead to electronic delocalization. In addition, to maintain local electroneutrality, the holes tend to be localized close to the lithium vacancies. Only when the number of holes and lithium vacancies increases (i.e., $x \leq 0.95$) is a metallic behavior found. This explains the drastic change of the conductivity and the phase transition, from a solid solution to a two phase domain in the x range 0.94−0.75.

This paper describes a combined in situ ac-impedance−X-ray diffraction study of the correlation between the electronic resistance (i.e., charge transport) and the structural properties (i.e., cell parameters) during the early stages of lithium deintercalation from $LiCoO_2$. The study has been performed using an electrochemical cell that permits in situ measurements of ac-impedance dispersions and X-ray diffraction spectra.

Experimental Section

$LiCoO_2$ (product no. 235-362-0, Merck battery grade) was used for all the measurements. The electrodes were prepared

* Address correspondence to either author. E-mail: fausto.croce@unich.it (F. C.); roberto.marassi@unicam.it (R. M.).
[†] Dipartimento di Scienze Chimiche, Università di Camerino.
[‡] Centro Interdipartimentale Grandi Apparecchiature.
[§] Dipartimento di Scienze del Farmaco, Università degli Studi.

10.1021/jp0606356 CCC: $33.50
Published on Web 05/18/2006

by spraying a dispersion of $LiCoO_2$−polyvinyl chloride (PVC, high molecular weight, Fluka)−acetylene black carbon (90:5:5 w/o) in THF onto a 10 μm thick high purity aluminum foil. The electrodes were dried at 120 °C under vacuum for at least 24 h before assembling the electrochemical cell. The electrode loadings were of the order of 1.5 mg/cm^2 of active mass.

The experimental cell used for the in situ measurements is a modification of the one developed by Ronci et al.[34] for in situ energy dispersive X-ray diffraction (EDXD). Basically, it consists of a thin walled (1 mm) polyethylene tube (10 mm i.d.) with threaded ends that accept removable screw cups holding two SS304 stainless steel rods acting as current collectors. The working electrode was shaped as a strip covered by the active compound in the central part and positioned on the top of the current collector. Two lateral wings, free of active compound, were bent around the sides of the current collector for the electrical contact. A polyethylene spacer was interposed between the top of the current collector and the active part of the working electrode in order to avoid any possible diffraction signal from the stainless steel. The counter electrode was a lithium disk pressed on the stainless steel current collector facing the working electrode. In some experiments a lithium wire was used as reference. The suitably insulated lithium wire was protruding from the center of the counter electrode shaped as a ring. Details on the cell construction can be found in ref 34. The electrolyte used was a 1 M $LiClO_4$ ethylene carbonate−dimethyl carbonate (EC−DMC 1:1, Merck battery grade). The electrodes were placed at a distance of about 5 mm; at this distance the X-ray diffracted beam can pass with no absorption by the counter electrode, and the electrodes are still quite close to each other to minimize the cell resistance.

The cell, assembled inside an argon filled drybox with moisture and oxygen content below 2 ppm, was cycled two times between 3.5 and 4.2 V at a very slow scan rate (C/20) to allow a proper SEI formation and properly sealed afterward. The electrochemical measurements were performed using a CHI660B electrochemical workstation by CH Instruments (Austin TX) driven by a PC. X-ray diffractogramms were collected in an angular dispersive X-ray diffraction (ADXD) configuration using a Rigaku Mo-Kα X-ray source equipped with a Huber goniometer. The sequence of operation consisted of a potentiostatic equilibration step at each potential followed by the acquisition of a diffractogramm at the pre-set potential and by the impedance measurement.

To maximize the diffraction by the sample and to minimize the interaction with the rest of the cell, the X-ray spectra were recorded with a grazing angle (2°) geometry. The electrochemical cell was kept at a fixed position and the detector was rotated in the 2θ range between 7.6 and 24° with 20 s steps of 0.02°. The impedance spectra were collected in the frequency region between 5 mHz and 100 kHz with 5 mV perturbation around the bias potential.

Results and Discussion

Figure 1 panel a shows a slow scan rate (10 μV/s) cyclic voltammogramm obtained using the cell in the two electrode configuration. The curve contains all the features expected for $LiCoO_2$.[15,16] The peak broadening and separation are caused by the un-compensated resistance due to the peculiar geometry of the cell used for in situ measurements. This demonstrates that the cell works properly from the electrochemical point of view. The curve was used, after integration, to compute the x value at each potential, as shown in Figure 1 panel b. Because of the uncertainty introduced by a slight capacity loss between first and second cycle due to partial solvent decomposition and SEI formation,[16] the calculated x values probably contain some bias and should be taken with some care.

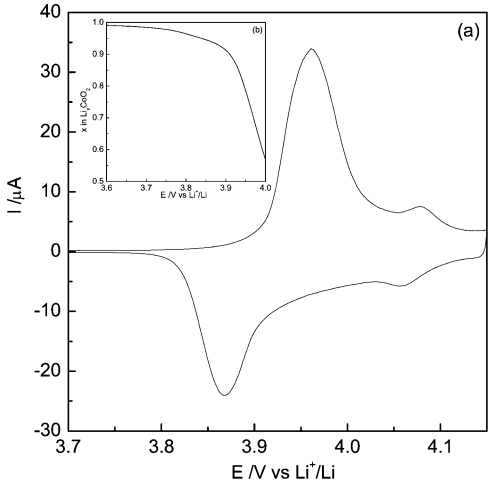

Figure 1. (a) Cyclic voltammogramm at very slow scan rate (10 μV s^{-1}) of the two-electrodes cell used for EIS and XRD measurements; (b) intercalation degree x as calculated from CV integration.

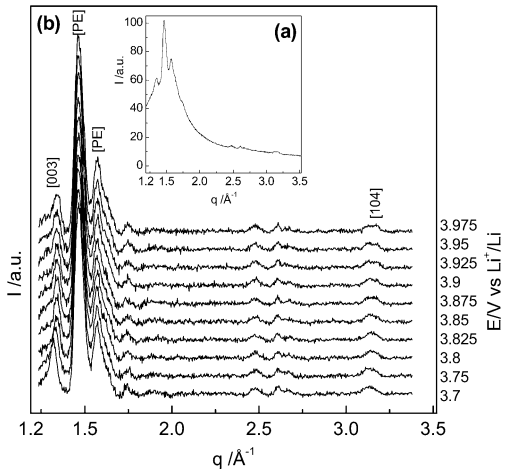

Figure 2. XRD in situ spectra: (a) at 3.7 V ($x = 0.99$) without any background subtractions; (b) at the selected potentials after background subtraction; main peaks of PE cell and active compound are indexed.

Figure 2 panel a shows a typical as-collected X-ray diffraction pattern at the starting potential of 3.7 V ($x \cong 1$). The broad background signal at low angles is due to the presence of liquid electrolyte. Figure 2 panel b shows the signals at different potential values after subtraction of the electrolyte background, simulated using a polynomial function. After this operation the spectra are still dominated by reflections mainly due to the polyethylene. To remove these contributions, the spectra have been further elaborated by subtracting the spectrum of the cell filled with the electrolyte. It is worth noting to this respect that the resolution of the resulting spectra is not significantly lower than that obtained by Ronci et al.[34] using *EDXD* configuration and an ordinary tungsten anode as source. Some smoothed spectra at different x values are shown in Figure 3. The spectra closely resemble previously published spectra of Li_xCoO_2[1−3,22,29]. The reflections can be indexed in the rombohedral system (space group R-3m) with cell parameters a and c equal to 2.815 and 14.049 Å, respectively, for $x = 1$. The low quality of the spectra, caused by overlapping reflections due to the active compound, liquid electrolyte, cell material, and collection geometry, prevents accurate refinement of the structural parameters. However, the main interest is, in this case, the relative variation

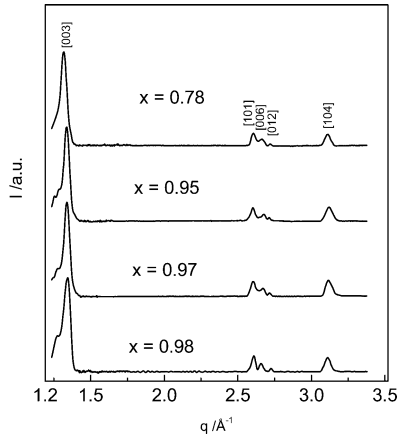

Figure 3. Smoothed X-ray spectra at selected x values after subtraction of the cell X-ray spectrum.

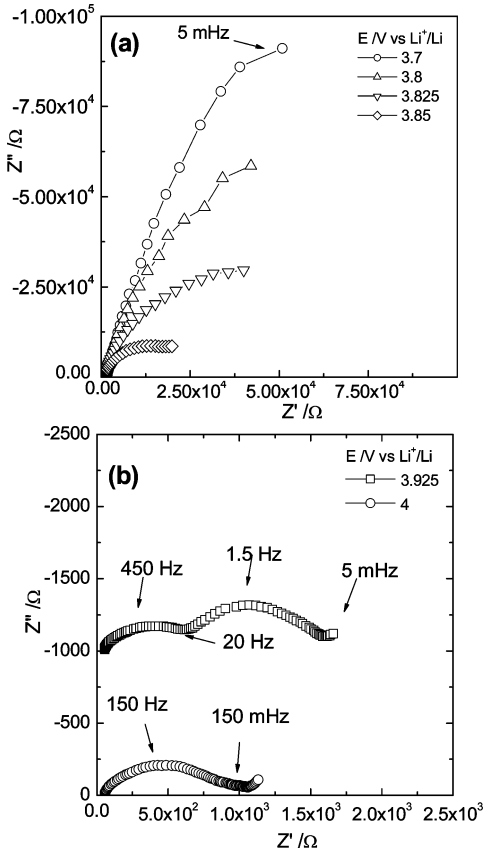

Figure 4. EIS dispersions at some significant intercalation levels (E = 3.7 V, x = 0.99; E = 3.8 V, x = 0.98; E = 3.825 V, x = 0.975; E = 3.85 V, x = 0.97; E = 3.925 V, x = 0.927; E = 4V, x = 0.71).

of the cell parameters with potential (i.e., intercalation degree x) and their comparison with the change of the ac-impedance main features. This has been proved to be possible as will be explained later on.

Figure 4 shows the ac-impedance dispersions recorded at some significant potentials corresponding to the X-ray spectra in Figure 2. The impedance dispersions shown have been taken using a two-electrode configuration and, hence, reflect both the contributions of the Li_xCoO_2 working electrode and of the lithium anode; however, the results shown in Figure 4, due to the negligible impedance of lithium electrode, do not differ significantly from those (not reported here) obtained with three-electrode configuration.

The dispersions show the same trend previously observed.[16] At low potentials (Figure 4a), the dispersions are dominated by a large, low-frequency, semi-circular arc that tends to close on the real axis as the deintercalation proceeds. At lower intercalation levels (Figure 4b), all other features that usually characterize the impedance spectra of this class of compounds are revealed: a 45° dispersion in the lowest-frequency region, a potential-dependent arc in the middle-to-low frequency region, an arc in the middle-frequency region that is almost invariant with the potential, and a small arc in the highest-frequency region that can be clearly seen only at higher magnification. All these features have been explained in previous papers[13−16] using an equivalent circuit that, using the Boukamp's notation[20], may be written as $R_{el}(R_{SEI}Q_{SEI})(Q_{dl}[R_{ct}(R_eQ_e)])Z_W]$[16] where R_{el} is the electrolyte resistance, $(R_{SEI}Q_{SEI})$ the solid electrolyte resistance with the associated capacity, Q_{dl}, R_{ct}, and Z_W have their usual meaning, and (R_eQ_e) is the electronic resistance with the associated capacity.

The equivalent circuit, discussed at length in ref 16, is a modification of the one proposed by Bruce and Saidi[35] for the intercalation of Li^+ in TiS_2 electrodes using the adatom model. The electrolyte resistance is in series with a parallel element that includes a Randles-type circuit to which a parallel (R_eQ_e) element has been added. In the original formulation, the latter parallel was composed by a resistance (R_{latt}, resistance to lattice incorporation) and a capacity (C_s, adatom−pseudo capacity) in series with an element (Z_{cpa}) to take into account the rough nature of the electrode.

As detailed in ref 16, the application of the adatom model to lithium intercalation has important consequences as far as, for instance, the charge transfer resistance is concerned. Basically, in the adatom model, the intercalation−deintercalation process is described in terms of partially desolvated lithium ions that are adsorbed on the electrode surface. The process is accompanied by the insertion of an electron into the conduction band of the host followed by diffusion of Li^+ to the intercalation site where it becomes fully incorporated into the lattice. The rate determining step is the incorporation of Li^+ ions into the lattice and, as a consequence, it follows that the charge-transfer resistance is potential independent. The model was developed for the case of intercalation in TiS_2 which is a good electronic conductor. For the Li_xCoO_2 system under examination, metallic conductivity is reached only for $x < 0.95$ and, hence, during the early stages of deintercalation the electron flow is limited by the low conductivity of the material, and the incorporation of lithium ions into the lattice is practically inhibited. In other words, electronic conduction and lithium ion lattice incorporation appear to be the rate-limiting steps of the overall charge-transfer process, respectively, for $x > 0.95$ and $x < 0.95$. Along this line, the parameter R_{latt} in the original equivalent circuit of Bruce and Saidi has been substituted by R_e, electronic resistance. The associated capacity Q_e includes the constant phase angle element that takes into account the rough nature of the electrode and the random orientation of crystallites inside active powder grains.[36]

If this interpretation is correct, the variations of the electronic resistance and of the cell structural parameters with x should be strictly correlated. This is especially true for the cell parameter a that corresponds to the in-plane R_{M-M} distance and that determines the insulating or metallic behavior of Li_xCoO_2. Figure 5c shows the variations of the electronic resistance, as deduced from the fitting of the ac-dispersion, and Figure 5a and b, those of the cell parameters c and a, respectively, derived

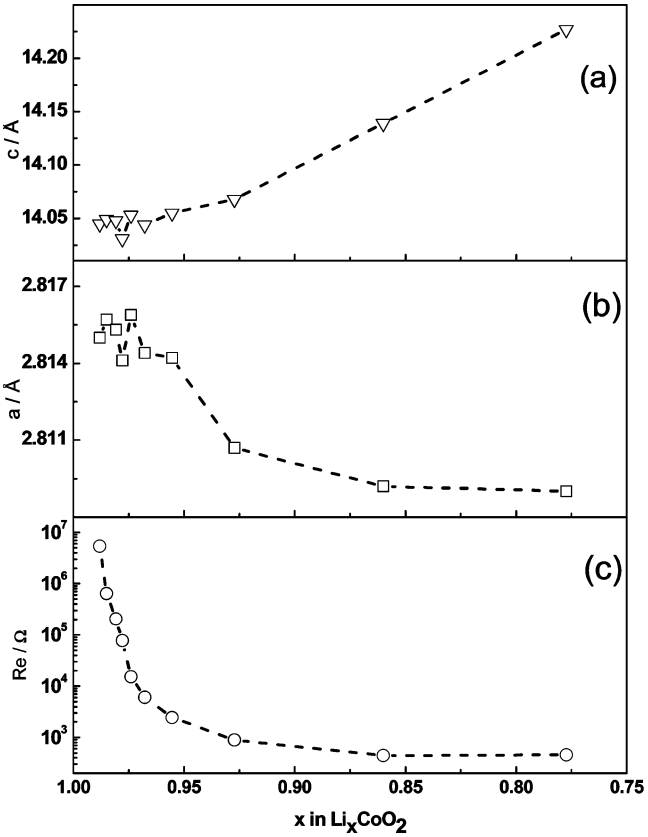

Figure 5. Comparison of electronic resistance (Re), *a*, and *c* cell parameters as a function of the intercalation degree.

by simulating the diffraction patterns as due to Bragg peaks of Gaussian shape using an in-house program vs the intercalation degree *x*.

As expected,[16] the electronic resistance decays sharply over a narrow *x* range reaching an almost constant value at *x* equal to about 0.9. The same trend is observed by the *a* parameter, while *c* shows a monotonic increase with decreasing *x*, in line with previously published results.[22,29] The direct comparison of structural and electrochemical results clearly demonstrates that the dramatic reduction of the cell impedance, that we have shown to be mainly related with the decrease of bulk electronic conductivity during the deintercalation process, occurs simultaneously with the contraction of the *a* parameter associated with the in-plane Co−Co distance and with the insulator-to-metal transition characteristic of the early stages of lithium deintercalation from $LiCoO_2$. In addition, the correlation of *a* and R_e, that reflects the physics of the process, confirms the validity of the adatom model for the intercalation−deintercalation process; i.e., the concomitant electronic diffusion and lithium ion incorporation into lattice that controls the rate of the overall charge-transfer mechanism for *x* ranging between 1 and 0.9.

Acknowledgment. This work was supported by Ministero dell'Istruzione dell'Università e della Ricerca (MIUR), Italy, PRIN 2003.

References and Notes

(1) Dahn, J. R.; von Sacken, U.; Jukow, M. R.; Al-Janabi, H. *J. Electrochem. Soc.* **1991**, *137*, 2207.
(2) Delmas, C.; Ménétrier, M.; Croguennec, L.; Saadoune, I.; Rougier, A.; Poullerie, C.; Prado, G.; Grüne, M.; Fournès, L. *Electrochim. Acta* **1999**, *45*, 243.
(3) Ueda, A.; Ohzuku, T. *J. Electrochem Soc.* **1994**, *141*, 2010.
(4) Arai, H.; Okada, S.; Sakurai, Y.; Yamaki, J. *J. Electrochem. Soc.* **1997**, *144*, 3117.
(5) Levi, E.; Levi, M. D.; Salitra, G.; Aurbach, D.; Oesten, R.; Heider, U.; Heider, L. *Solid State Ionics* **1999**, *126*, 97.
(6) Delmas, C.; Saadounne, I.; Rougier, A. *J. Power Sources* **1993**, *43*−*44*, 595.
(7) Croce, F.; Deptula, A.; Lada, W.; Marassi, R.; Olczak, T.; Ronci, F. *Ionics* **1997**, *3*, 390.
(8) Ohzuku, T.; Ueda, A. *J. Electrochem Soc.* **1997**, *144*, 2780.
(9) Mizushima, K.; Jones, P. C.; Wiseman, P. J.; J. B. Gooedenough *Mater. Res. Bull.* **1980**, *15*, 783.
(10) Megahed, S.; Scrosati, B. *J. Power Sources* **1994**, *51*, 79.
(11) Dokko, K.; Mohamedi, M.; Fujita, Y.; Itoh, T.; Nishizawa, M.; Umeda, M.; Uchida, I. *J. Electrochem Soc.* **2001**, *148*, A422.
(12) Levi, M. D.; Gamolsky, K.; Aurbach, D.; Heider, U.; Oesten, R. *Electrochim. Acta* **2000**, *45*, 1781.
(13) Croce, F.; Nobili, F.; Deptula, A.; Lada, W.; Tossici, R.; D'Epifanio, A.; Scrosati, B.; Marassi, R. *Electrochem. Comm.* **1999**, *1*, 605.
(14) Nobili, F.; Tossici, R.; Croce, F.; Scrosati, B.; Marassi, R. *J. Power Sources* **2000**, *98*, 238.
(15) Nobili, F.; Croce, F.; Scrosati, B.; Marassi, R. *Chem. Mater.* **2001**, *13*, 1642.
(16) Nobili, F.; Tossici, R.; Marassi, R.; Croce, F.; Scrosati, B. *J. Phys. Chem. B* **2002**, *106*, 3909.
(17) Levasseur, S.; Ménétrier, M.; Suard, E.; Delmas, C. *Solid State Ionics* **2000**, *128*, 11.
(18) Aydinol, M. K.; Kohan, A. F.; Ceder, G.; Cho, K.; Joannopoulos, J. *Phys. Rev. B* **1997**, *56*, 1354.
(19) Shibuya, M.; Nishina, T.; Matsue, T.; Uchida, I. *J. Electrochem Soc.* **1996**, *143*, 3157.
(20) Boukamp, B. A. *Solid State Ionics* **1986**, *20*, 159.
(21) Cho, J.; Jung, H. S.; Park, Y. C.; Kim, G. B.; Lim, H. S. *J. Electrochem. Soc.* **2000**, *147*, 15.
(22) Ménétrier, M.; Saadoune, I.; Levasseur, S.; Delmas, C. *J. Mater. Chem.* **1999**, *9*, 1135.
(23) Nishizawa, M.; Yamamura, S.; Itoh, T.; Uchida, I. *Chem. Commun.* **1998**, *16*, 1631.
(24) Sato, H.; Takahashi, D.; Nishina, T.; Uchida, I. *J. Power Sources* **1997**, *68*, 540.
(25) Van der Ven, A.; Aydinol, M. K.; Ceder, G.; Kresse, G.; Hafner, J. *Phys. Rev. B* **1998**, *58*, 2975.
(26) Van der Ven, A.; Aydinol, M. K.; Ceder, G. *J. Electrochem. Soc.* **1998**, *145*, 2149.
(27) Koyama, Y.; Kim, Y. S.; Tanaka, I.; Adachi, H. *Jpn. J. Appl. Phys.* **1999**, *38*, 2024.
(28) Koyama, Y.; Tanaka, I.; Kim, Y. S.; Nishitani, S. R.; Adachi, H. *Jpn. J. Appl. Phys.* **1999**, *38*, 4804.
(29) Reimers, J. N.; Dahn, J. R.; *J. Electrochem. Soc.* **1992**, *139*, 2091.
(30) Goodenough, J. B. In *Progress in Solid State Chemistry;* Reiss, H., Ed.; Pergamon Press: Oxford, 1971; Vol 5, p 279.
(31) Molenda, J.; Stoklosa, A.; Bak, T. *Solid State Ionics* **1989**, *36*, 53.
(32) Molenda, J. *Phys. Status Solidi B* **1989**, *165*, 419.
(33) Molenda, J. *Solid State Ionics* **1999**, *119*, 19.
(34) Ronci, F.; Scrosati, B.; Rossi Albertini, V.; Perfetti, P. *J. Phys. Chem. B* **2001**, *105*, 754.
(35) Bruce, P. G.; Saidi, M. Y. *J. Electroanal. Chem.* **1992**, *322*, 93.
(36) Granquist, C. G. *Appl. Phys. A* **1993**, 57, 32.